PERGAMON

Deep-Sea Research I 46 (1999) 831–854

DEEP-SEA RESEARCH
PART I

Sensitivity of ^{234}Th export to physical processes in the central equatorial Pacific

John P. Dunne*, James W. Murray

School of Oceanography, Box 357940, University of Washington, Seattle, WA 98195-7940, USA

Received 30 September 1997; received in revised form 21 April 1998; accepted 27 July 1998

Abstract

We determined the sensitivity of the calculated sinking flux of ^{234}Th in the central equatorial Pacific to physical processes and scavenging mechanisms by imposing a meridional and vertical advection and diffusion field on a simple dissolved and particulate ^{234}Th cycle. We used the model to estimate the efficiency with which the ^{234}Th deficiency relative to ^{238}U reflected the predicted sinking flux of ^{234}Th on particles and compared our results with ^{234}Th data taken during the JGOFS-EqPac 1992 Survey II Cruise. ^{234}Th deficiencies near the equator were strongly affected by both vertical advection and horizontal diffusion. The model ^{234}Th deficiency at the equator underestimated the model ^{234}Th sinking flux by 144% in neglecting advection and diffusion in the presence of strong upwelling at the equator. The model ^{234}Th deficiency at the equator corrected for advection overestimated the sinking flux of ^{234}Th by 33% in neglecting horizontal diffusion. Analysis of the scavenging mechanism suggests that, during situations of export governed by rapidly sinking particles, ^{234}Th-based estimates of particle export are only half as sensitive to advection compared to situations of export governed by slowly sinking particles. Given that results using the mechanism of slowly sinking particles compare better with the observed ^{234}Th deficiency and calculated meridional ^{234}Th fluxes at the equator than the mechanism of rapidly sinking particles, we consider the mechanism of slowly sinking particle more appropriate for this region. In agreement with previous studies based on observed ^{234}Th gradients, this study supports the incorporation of vertical advection terms in the ^{234}Th balance to estimate particulate carbon export at the equator but suggests that this method may have overestimated the sinking flux at the equator during EqPac Survey II by 0–63% due to the role of horizontal diffusion.

* Corresponding author. E-mail: jdunne@ocean.washington.edu

0967-0637/99/$ – see front matter
PII: S0967-0637(98)00098-3

1. Introduction

^{234}Th is a tracer of particle transport and cycling in the surface ocean (Coale and Bruland, 1985). The ^{234}Th method consists of using the water column deficiency of ^{234}Th relative to ^{238}U to calculate the sinking flux of ^{234}Th due to particle scavenging. In one application of this method, the calculated sinking flux of ^{234}Th is multiplied by the C:^{234}Th ratio in sinking particles to obtain the sinking flux of carbon (Buesseler et al., 1992, 1994, 1995; Bacon et al., 1996; Murray et al., 1996). If the concentration of ^{234}Th in sinking particles is known, the sinking flux of ^{234}Th can be used to estimate the average sinking velocity of particles (Buesseler et al., 1995; Bacon et al., 1996; Dunne et al., 1997). A second application of the ^{234}Th method is to use the ratio of the calculated sinking flux of ^{234}Th to the measured ^{234}Th flux in sediment traps to correct sediment traps for hydrodynamic biases (Murray et al., 1996). For both approaches, it must be shown (or assumed) that ^{234}Th and carbon are transported by the same particles (Murray et al., 1996).

The accuracy of the ^{234}Th method depends highly on the accuracy of the ^{234}Th deficiency as a diagnostic of the ^{234}Th sinking flux. It is thus important to determine the contribution of advection and diffusion to the calculated ^{234}Th flux, but this is usually difficult to accomplish due to a lack of spatial resolution in the data and weak physical constraints. Fortunately, both of these limitations can be addressed using data from the US JGOFS Process Study in the central equatorial Pacific (EqPac; Murray et al., 1994).

The central equatorial Pacific is well recognized as a regime of intense circulation in which the easterly trade winds drive equatorial divergence (Wyrtki and Kilonsky, 1984). Though zonal currents are stronger than vertical and meridional currents in the upper 300 m, recent model studies have shown that vertical and meridional circulation dominates tracer budgets due to the strength of divergence relative to the long zonal extent of the region. Liu et al. (1994) found that a typical water parcel is upwelled at the equator in the east and recirculated meridionally 3–6 times while traversing zonally from east to west across the Pacific.

Extensive studies of ^{234}Th were recently conducted in the equatorial Pacific as part of EqPac (Buesseler et al., 1995; Murray et al., 1996; Bacon et al., 1996). The combination of these ^{234}Th data and relatively well-defined physics in the central equatorial Pacific allowed investigation of the advective components of the ^{234}Th balance. In these studies the effect of advection on calculations of ^{234}Th flux was estimated using advection velocities generated from general circulation model results of Chai (1995). Qualitatively, these studies showed that vertical and meridional advection had a major effect on the ^{234}Th flux balance and on calculations of the flux of ^{234}Th from the upper water column. For example, Murray et al. (1996) suggested that at the equator the flux of ^{234}Th into the surface due to upwelling was about half the downward flux of ^{234}Th on particles. Buesseler et al. (1995) reported that vertical advective fluxes at the equator were approximately equal to the radioactive deficiency flux while zonal fluxes were generally less than 5% and always less than 25% of the radioactive deficiency flux. A general lack of zonal ^{234}Th gradients was also observed on the recent FLUPAC and Zonal Flux cruises along the equator from 165°E to

150°W (J.P. Dunne et al., submitted). Results from these studies showed that ^{234}Th scavenging and vertical advection had similar magnitudes of opposing impact on the ^{234}Th flux balance in the equatorial surface ocean while zonal advection was negligible. These fluxes, however, were calculated by multiplying observed gradients in ^{234}Th times the flow field and have large relative errors, generally over 100%, leading to a large uncertainty in the advection-corrected ^{234}Th flux balance. In addition, these studies did not estimate the impact of diffusion.

The geochemical importance of ^{234}Th is its potential as a method for predicting the export flux of particulate carbon and calibrating sediment traps (Buesseler, 1991). The focus of this study is to critically evaluate the sensitivity of the ^{234}Th method to circulation in the central equatorial Pacific and assess the uncertainty in the ^{234}Th method as a calibration tool for sediment traps. We calculated ^{234}Th fluxes due to scavenging, advection and diffusion on a two-dimensional flow field adopted from general circulation models to evaluate the sensitivity of the modeled ^{234}Th flux to radvection and diffusion. This method has the advantage of being numerically fully consistent and exact and allowed us to look at the individual effect of each process on the ^{234}Th flux balance. In this paper we present model predictions which show that: (1) Vertical advection at the equator has a dramatic effect on the ^{234}Th flux balance such that vertical advection must be incorporated into ^{234}Th-based estimates of export. (2) Horizontal diffusion also has a significant effect on ^{234}Th flux balance such that ^{234}Th-based export estimates corrected only for advection overestimate the sinking flux by up to 63%. (3) A scavenging mechanism involving rapid particle sinking predicts that advection and diffusion are only approximately half as important to the ^{234}Th mass balance as does one involving slow particle sinking.

2. Model description

We simplified the conceptual model of equatorial circulation (e.g. Philander, 1990) in order to simulate only the most essential components of the complex four-dimensional circulation in the central equatorial Pacific. These components are equatorial upwelling and meridional recirculation. A two-dimensional advection stream function of upwelling and meridional recirculation between the equator and 5°N and 5°S was patterned after the vertical advection fields of Liu et al. (1994) and Chai (1995).

We then superimposed the thorium scavenging model of Bacon and Anderson (1982) on the circulation field. The thorium scavenging model was a two-component model shown schematically in Fig. 1 in which dissolved ^{234}Th, Th_d, undergoes first-order, reversible sorption to become particulate ^{234}Th, Th_p, which sinks through the water column. As discussed above, zonal gradients and subsequently zonal advective and diffusive fluxes have been shown to be small and can be neglected. Ignoring these zonal terms, the continuity equations for dissolved and particulate ^{234}Th are:

$$\partial Th_d/\partial t = U\lambda - (\lambda + k_1')\,Th_d + k_{-1}\,Th_p - v\partial Th_d/\partial y - w\partial\, Th_d/\partial z + (\partial K_h(\partial Th_d/\partial y))/\partial y + (\partial K_z(\partial Th_d/\partial z))/\partial z, \quad (1)$$

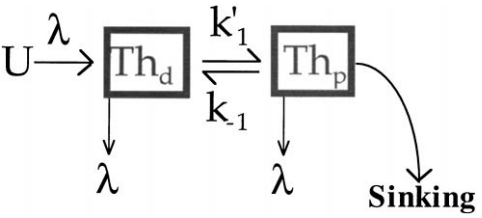

Fig. 1. Diagram of the thorium scavenging model (Bacon and Anderson, 1982), where boxes indicate reservoirs and arrows indicate fluxes.

$$\partial Th_p/\partial t = k'_1\, Th_d - (\lambda + k_{-1})\, Th_p - (S + w)\partial Th_p/\partial z - v\partial Th_p/\partial y + (\partial K_h(\partial Th_p/\partial y))/\partial y + (\partial K_z(\partial Th_p/\partial z))/\partial z. \quad (2)$$

All parameters used in this study are described in Table 1. We assumed single values of the ^{234}Th decay constant (λ), desorption rate constant (k_{-1}) and horizontal diffusion constant (K_h), two values of the vertical diffusion constant (K_z), and fields of meridional (v) and vertical (w) advection as described below. We estimated the apparent adsorption rate constant (k'_1) and sinking velocity (S) from the dissolved ^{234}Th (Th_d), particulate ^{234}Th (Th_p) and total ^{238}U (U) data also described below.

Data for Th_t (Murray et al., 1996) and Th_d (Dunne et al., 1997) were taken during JGOFS-EqPac Survey II (π011;http://www1.whoi.edu/jgofs.html; Fig. 2A and B). Th_p was calculated as the difference between Th_t and Th_d (Fig. 2C). Model output was evaluated by its ability to reproduce the following key features observed in the EqPac Survey II data: (1) uniformly low levels of Th_t in the mixed layer, (2) secular equilibrium levels of Th_t at 200–250 m, (3) Th_p levels approximately a third of the Th_d levels and (4) Th_p levels that have their maximum in or directly below the mixed layer and decrease at greater depth.

3. Model parameterization

We used a two-dimensional steady-state model with a meridional resolution of 1/8° and a vertical resolution of 10 m to evaluate the effect of a hypothetical advection and diffusion regime on distributions of ^{234}Th. Calculating model fluxes at steady state allowed us to obtain an exact solution without uncertainties due to numerical diffusion or dispersion. The numerical scheme was set up as a steady-state flux inventory using a staggered grid such that for any compartment, inventories of ^{234}Th were defined within the compartment and velocities at each corner. This scheme was chosen because it conserves fluxes in areas where diffusion coefficients change, such as at the base of the model's mixed layer. After all parameters were set, the matrix of equations was inverted to obtain distributions of dissolved and particulate ^{234}Th.

Our two-dimensional advection stream function for meridional and vertical velocity was modeled after the work of Chai (1995), which used the modular ocean model

Table 1
Summary of parameters used in the scavenging/two-dimensional circulation model

Symbol	Definition	Units	Description
U	Total ^{238}U activity	dpm m^{-3}	$U_{data} = 0.0686$. Salinity $(1 + \sigma_\theta/1000)$; $U_{model} = 2440$
Th_t	Total ^{234}Th activity	dpm m^{-3}	Unfiltered Go-Flo samples
Th_d	Dissolved ^{234}Th activity	dpm m^{-3}	Go-Flo samples passing a 0.4 μm filter
Th_p	Particulate ^{234}Th activity	dpm m^{-3}	$Th_p = Th_t - Th_d$
P	particle concentration	mmol C m^{-3}	CTD beam attenuation multiplied by 18.547
λ	decay constant	d^{-1}	$\lambda = 0.02876$
k_{-1}	desorption constant	d^{-1}	$k = 0.0068$, Clegg and Whitfield (1993)
k_1'	apparent adsorption constant	d^{-1}	Calculated from data using Eq. (3)
v	meridional velocity	°lat d^{-1}	Stream function after Chai (1995) and Liu et al., (1994)
w	vertical velocity	m d^{-1}	Stream function after Chai (1995) and Liu et al., (1994)
K_h	horizontal diffusion coefficient	°lat^2 d^{-1}	$K_h = 0.007$ (Pacanowski and Philander, 1981)
K_z	vertical diffusion coefficient	m^2 d^{-1}	$K_z = 2450$ above 70 m and $K_z = 2.6$ (Pacanowski and Philander, 1981) below 70 m
k_1	inherent adsorption constant	mmol C^{-1} m^3 d^{-1}	Calculated from regression of k_1' against P
S	sinking velocity	m d^{-1}	Calculated by tuning model to the observed deficiency
R_{def}	deficiency flux : sinking flux ratio	—	Calculated by integrating the model deficiency to 120 m and dividing by SP_{120}
$R_{def+adv}$	deficiency and advection flux: sinking flux ratio	—	Calculated by integrating the model deficiency to 120 m adding advection terms and dividing by SP_{120}

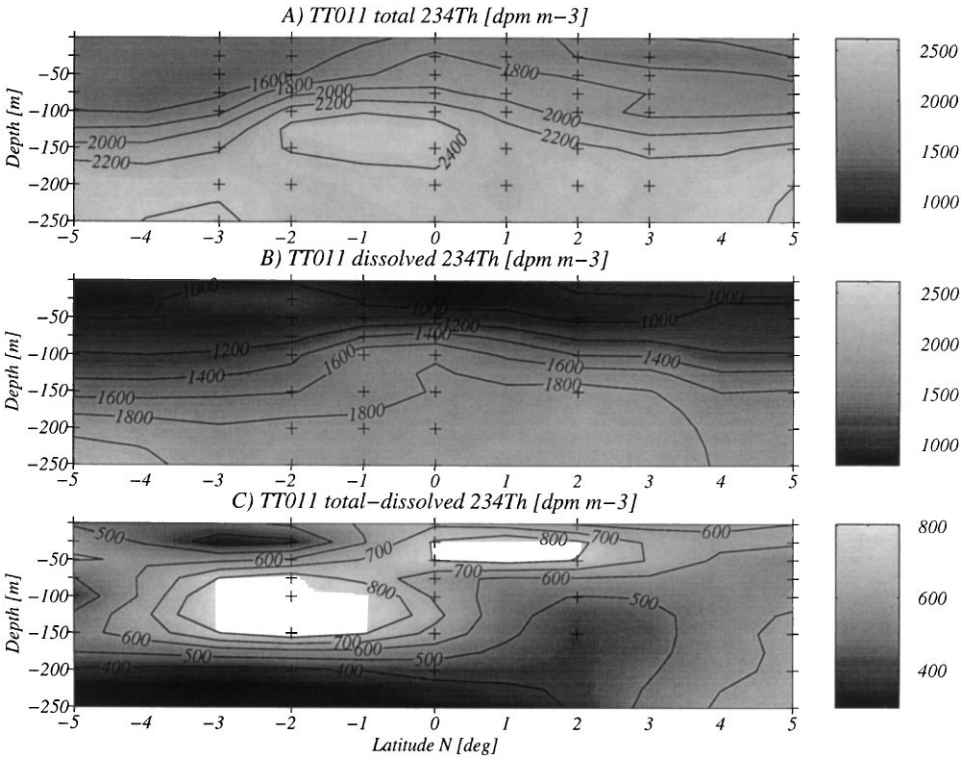

Fig. 2. Data contours of total ^{234}Th (2A) dissolved ^{234}Th (2B) and particulate ^{234}Th (= total − dissolved; 2C) (dpm m^{-3}) between 5°N and 5°S in the upper 250 m from JGOFS-EQPAC Survey II (π011).

(MOM) forced by the COADS winds observed during September–November of 1992, and after the work of Liu et al. (1994), which was forced by climatological winds. The stream function was a set of empirical, exponential functions combined to give streamlines of velocity. The empirical equations for meridional (v) and vertical (w) velocity are:

$$v = (1 - e^{-0.35y})(5.125 - y)(0.22(e^{-z/50} - e^{-290/50} - z/50e^{-z/50}) - 6.4(\pi/290\cos(z\pi/290)(e^{-z/120} - e^{-290/120}) - \sin(z/290\pi)/120e^{(-z/120)})),$$

$$w = (z(e^{-z/50} - e^{-290/50})0.22 - 6.4\sin(\pi z/290))(e^{-z/120} - e^{-290/120}) \times (0.35e^{(-0.35y)})(5.125 - y) - 1 - e^{(-0.35y)})$$

where y and z are the meridional (° latitude) and vertical (meters) coordinates. Contour plots of v and w are shown in Fig. 3. Zonal advection was neglected in this model. Liu et al. (1994) gave a detailed climatological analysis of the relative features of equatorial and tropical circulation, showing that water upwelled at the equator was

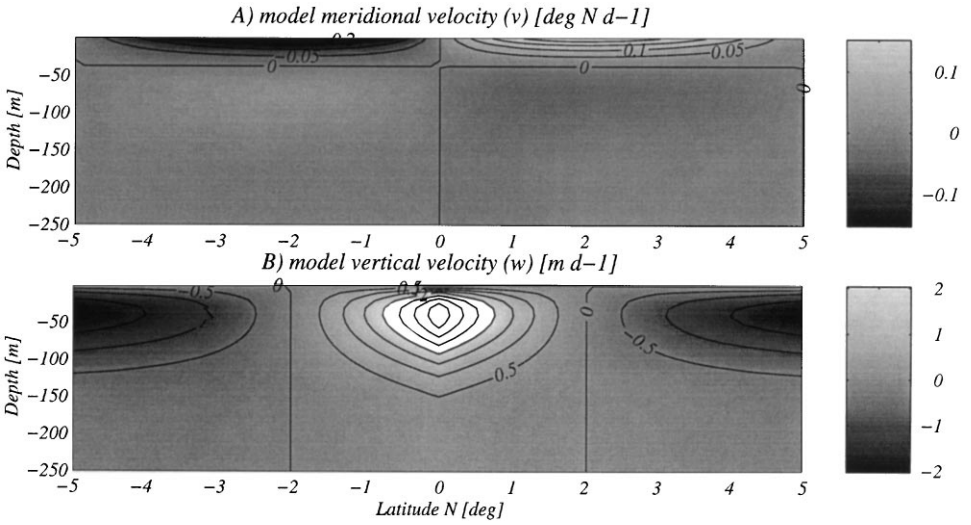

Fig. 3. Contours of meridional velocity (A) (°N d^{-1}) and vertical velocity (B) (m d^{-1}) between 5°N and 5°S in the upper 250 m from the empirical stream function.

primarily associated with intense meridional recirculation rather than meridional export past 5°N and 5°S. Chai (1995) used a less detailed numerical model forced by actual winds to estimate upwelling conditions during EqPac Survey II. He found an upwelling velocity at the equator of 4 m d^{-1} at 50 m. Upwelling decreased to 1 m d^{-1} at the base of the euphotic zone (120 m) and to zero vertically below 150 m and horizontally at 2°N and 2°S. For simplicity, the circulation was assumed to be symmetric about the equator and thus does not reflect the true meridional asymmetry observed in this region that is caused by the presence of the Inter-tropical Convergence Zone north of the equator (Philander, 1990). The shapes of the contours of upwelling velocity (Fig. 3B) were tuned to reproduce the features in Chai (1995) described above. Circulation was also assumed to be closed between the equator and 5° north and south. The work of Liu et al. (1994) suggested that about 25% of the meridional flow along the surface escapes recirculation. More recent work by Lu et al. (1998) suggested that this flow could be as much as 70%. These studies imply that the model used here overestimates downwelling velocities between 2° and 5° by 25–70% relative to upwelling velocities at the equator. As our focus here is on the equator, not on the 2–5° region, we do not consider this uncertainty a critical flaw in the model but note it as a word of caution.

Estimates of diffusion in the literature vary over a considerable range depending on the time and space scales (i.e. magnitudes of convection) that the measurements integrate over. Horizontal diffusion estimates range from 3 m^2 s^{-1} from a tracer release experiment in the south Pacific (Ledwell, 1993) to 5000 m^2 s^{-1} from a larger scale helium–tritium mass balance in the tropical Pacific (Fine and Ostlund, 1980). Similarly, estimates of vertical diffusion in the literature vary over an order of magnitude

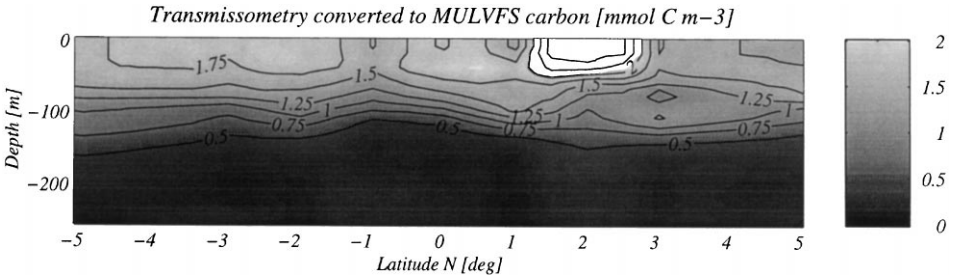

Fig. 4. Data contour of beam attenuation (mmol C m^{-3}) between 5°N and 5°S in the upper 250 m during JGOFS-EQPAC Survey II normalized to particulate carbon from Bishop (in press).

between microscale and tracer release estimates of 0.1 $cm^2 s^{-1}$ (e.g. Ledwell, 1993) and tracer budget estimates of 1–2 $cm^2 s^{-1}$ (e.g. Munk, 1966). For this study we set $K_h = 1000\ m^2 s^{-1}$ ($= 0.007°lat^2 d^{-1}$) and $K_z = 0.3\ cm^2 s^{-1}$ ($= 2.6\ m^2 d^{-1}$) below the mixed layer, consistent with Pacanowski and Philander (1981). A constant mixed layer with a depth of 70 m obtained from the EqPac Survey II average (using the density change of 0.125; Gardner et al., 1996) was set to mix once per day with a vertical diffusion coefficient of 0.028 $m^2 s^{-1}$ ($=2450\ m^2 d^{-1}$).

Estimates of particle concentration (P) were obtained from CTD beam attenuation (http://www1.whoi.edu/jgofs.html; Fig. 4). To express P in more convenient units, beam attenuation was converted to particulate organic carbon concentration units using a factor of 18.5 mmol C m^{-2} calibrated from the Multiple Unit Large Volume Filtration System (MULVFS) data of J.H. Bishop (in press). The ^{234}Th decay constant (λ) was set to 0.02876 d^{-1}, and the desorption rate constant (k_1) was set to 0.0068 d^{-1} after the compilation of Clegg and Whitfield (1993).

For the model to predict the distributions of ^{234}Th, the apparent adsorption rate constant (k_1') had to be estimated for each grid cell. Though k_1' can be calculated directly from the data for some cells and then interpolated for the others, the resulting field is extremely noisy due to analytical uncertainty. We chose to minimize these complications by parameterizing k_1' in the model, taking advantage of the strong correlation observed here and elsewhere between k_1' and P (Bacon and Anderson, 1982; Honeyman et al., 1988; Dunne et al., 1997). We assumed a first order relationship between k_1' and P ($k_1' = k_1 P$) to parameterize the adsorption field in the model using a three-step process. In the first step, Eq. (1) was re-arranged into Eq. (3) to obtain estimates of k_1' from the EqPac Survey II data using Th_d and Th_p shown in Fig. 2 and U calculated from salinity and density ($U = 0.0686S(1 + \sigma_\tau/1000)$; Murray et al., 1996). Estimates of v and w were taken from Chai (1995). As analytical uncertainty in Th_d was too high to estimate second derivatives, diffusion terms were neglected.

$$k_1' = \frac{\left(\lambda(U - Th_d) + k_{-1} Th_p - v\frac{\partial Th_d}{\partial y} - w\frac{\partial Th_d}{\partial z}\right)}{Th_d}. \tag{3}$$

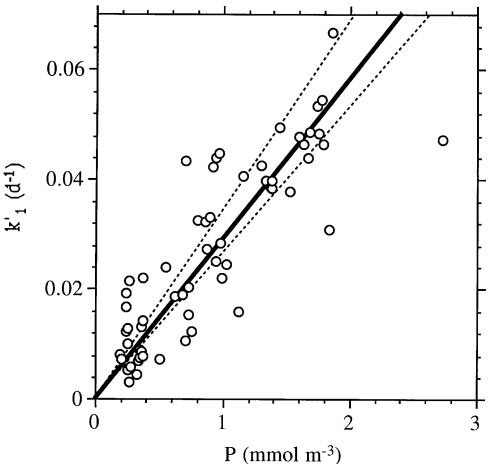

Fig. 5. Estimates of the adsorption rate constant, k'_1 (d^{-1}), versus particle concentration, P (mmol C m^{-3}), from beam attenuation using the data from JGOFS EQPAC Survey II in Figs. 2 and 4. Also shown is the fixed-intercept regression (solid line with slope = 0.02905 mol C^{-1} m^3 d^{-1}; Mood, 1950) with its 95% confidence interval of 0.0266–0.0343 mmol C^{-1} m^3 d^{-1} (dotted lines). Assuming $k'_1 = k_1 P$, the slope gives the value for k_1.

In the second step, values of k'_1 were regressed against P (Fig. 5) to obtain an inherent adsorption rate constant (k_1) from the slope. Variability in P was able to explain 73% of the variability in k'_1, giving us great confidence in the parameterization. We estimated the most probable slope ($k_1 = 0.02905$ mmol C^{-1} m^3 d^{-1}) and its 95% confidence intervals (0.0266–0.0343 mmol C^{-1} m^3 d^{-1}; $n = 60$) using Mood's non-parametric method (Mood, 1950). Mood's method has three advantages: (1) It weights ranks, eliminating biases due to extreme values. (2) It enables the straightforward calculation of confidence intervals. (3) It allows the intercept to be fixed (to zero in this case). Thirdly, the model field of k'_1 was obtained through multiplying k_1 by P (Fig. 4) in each grid cell.

Boundary conditions for the model were zero flux across all boundaries except along the bottom where Th_p was allowed to vary. The model activity field of ^{238}U was set everywhere to 2440 dpm m^{-3}. The model sinking velocity (S) was used as an adjustable parameter to minimize the difference between observed and modeled ^{234}Th deficiencies in the upper 120 m (Fig. 9A). The 0–120 m depth interval was chosen for this calculation to assure consistency with the JGOFS-EQPAC flux normalization protocol to a 120 m euphotic zone defined by the 0.1% light level (Murray et al., 1996). This minimization procedure gave a sinking velocity of $S = 3.01$ m d^{-1} with a 93% confidence interval of 2.51–3.59 m d^{-1}. At the chosen sinking velocity, the observed and modeled deficiencies agree within 10% on average. The value of $S = 3.01$ m d^{-1} was used for all model runs except in the sinking velocity sensitivity analysis.

4. Results and discussion

4.1. Discussion of modeled ^{234}Th distributions

Our primary goal was to determine the effect of advection and diffusion on the ^{234}Th deficiency and thus the calculated ^{234}Th sinking flux. To this end we considered primarily distributions of total ^{234}Th (= dissolved + particulate), because the distribution of total ^{234}Th determines the ^{234}Th deficiency. Here we present model fields of total ^{234}Th, first from the chemical model alone without any physical terms and then with the inclusion of each term individually to illustrate its impact. Neglecting both advection and diffusion gave the distributions shown in Fig. 6A. ^{234}Th increased almost linearly with depth between the surface and 150 m to values in equilibrium with ^{238}U. This broad, linear increase in ^{234}Th with depth was unlike the sharp vertical front in ^{234}Th at the base of the mixed layer that was actually observed (Fig. 2A). Adding horizontal and vertical diffusion without advection gave the contour plot shown in Fig. 6B. In this case total ^{234}Th was uniformly low in the mixed layer and increased linearly between 70 and 150 m. The striking contrast between Fig. 6A and B in the upper 70 m illustrates the importance of the mixed layer in homogenizing upper ocean ^{234}Th activities in the central equatorial Pacific. Adding advection without diffusion produced contours of ^{234}Th that bowed upward at the equator and spread downward at higher latitudes (Fig. 6C). In addition, the process of adsorption and sinking (and to a small degree subsequent desorption) at the equator had a focusing effect, creating extremely high values of ^{234}Th in the vertical zone where particulate ^{234}Th was high. This feature is further discussed below.

The combined effects of advection and diffusion are shown in Fig. 6D. The addition of a mixed layer removed much of the vertical structure; horizontal mixing broadened and smoothed the meridional extent of high surface ^{234}Th due to upwelling. Mixed layer values near the equator were elevated, and levels at high latitudes were depressed relative to the diffusion-alone case (Fig. 6B). The strong subsurface maximum observed in Fig. 6C at the equator was replaced by a much weaker subsurface maximum at 125 m, which was displaced slightly to the north. This northward displacement of the maximum was because the highest particle concentrations observed at 2°N (Fig. 4) led to the highest predicted values of k_1'. Diffusion smeared the features at the equator and at 2°N. The model results for total ^{234}Th in Fig. 6D can be compared directly with the data for total ^{234}Th in Fig. 2A for a qualitative assessment of the model. The model reproduced both the patterns and magnitudes observed in the data including the mixed layer levels, the equatorial surface maximum and the equatorial subsurface maximum. On average, modeled total ^{234}Th activities were within 11% of the data and reproduced 76% of the variability.

We compare each source and removal term in the ^{234}Th flux balance in the upper 120 m in Fig. 7. The ^{234}Th deficiency, the difference between the U and Th_t decay fluxes, is shown instead of the absolute fluxes for ease in comparison with the other terms. Except at the equator, the deficiency and the sinking flux were of similar magnitude (opposite in sign). Upwelling at the equator inputs high ^{234}Th into the upper 120 m, making vertical advection a large positive flux and resulting in a smaller

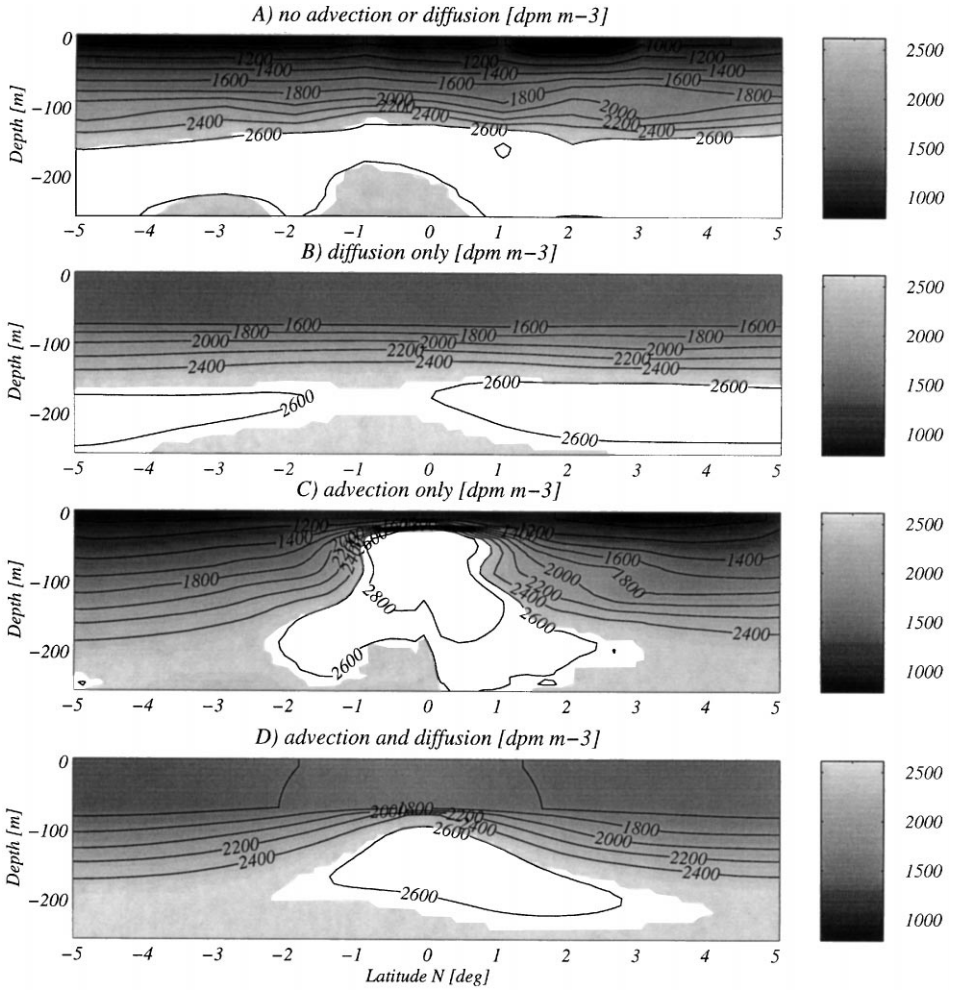

Fig. 6. Model contours of total ^{234}Th (dpm m^{-3}) between 5°N and 5°S in the upper 250 m from the two dimensional model without advection or diffusion (A), with diffusion but no advection (B), with advection but no diffusion (C) and with advection and diffusion (D).

^{234}Th deficiency from ^{238}U. Vertical advection was thus an important part of the ^{234}Th flux balance at the equator. This result confirms previous studies. Horizontal diffusion carried some of this high ^{234}Th away from the equator. The important role of horizontal diffusion on the ^{234}Th flux balance at the equator was not previously accounted for. Off the equator horizontal advection carried an additional amount further away. Vertical diffusion across the base of the euphotic zone (120 m) was everywhere a small factor and was not an important part of the ^{234}Th flux balance. This was also not previously known. It should be noted that this is only true in regions of the ocean such as the equatorial Pacific where the mixed layer is shallower than the

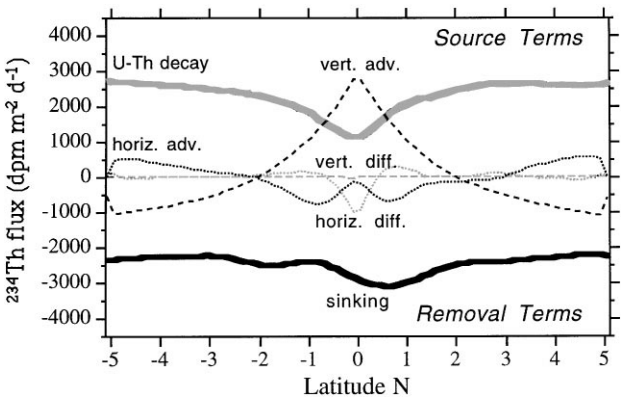

Fig. 7. Model diagnostic summary of the ^{234}Th flux balance (0–120 m) versus latitude showing: the difference between ^{238}U and ^{234}Th decay (the deficiency; thick gray), particle sinking (thick black), vertical advection (dashed black), horizontal advection (dotted black), vertical diffusion (dashed gray) and horizontal diffusion (dotted gray).

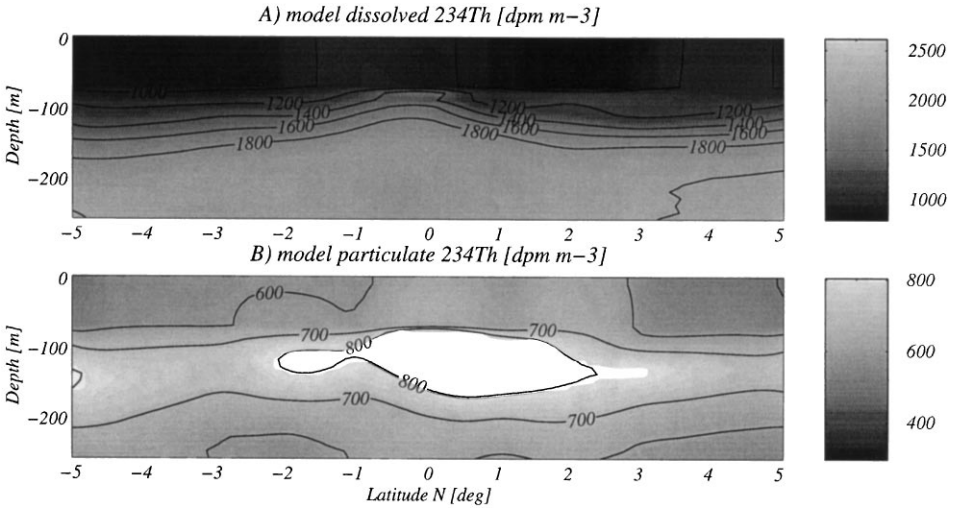

Fig. 8. Model contours of dissolved (A) and particulate (B) ^{234}Th (dpm m^{-3}) between 5°N and 5°S in the upper 250 m from the two-dimensional model with advection and diffusion.

depth of the euphotic zone. The model gave significant negative advective fluxes between 2 and 5° due to downwelling. Because the model did not allow any water to leave at the surface to the north and south, it overestimated downwelling at high latitudes relative to upwelling at the equator.

The model Th_d distribution (Fig. 8A) compared well with the data (Fig. 2B), reproducing the surface low and linear subsurface increase. It showed a similar overall

pattern as for modeled Th_t (Fig. 6D) except that the model Th_d lacked a subsurface maximum. On average, modeled Th_d activities were within 6.3% of the data and reproduced 85% of the variability.

The distribution of modeled Th_p (Fig. 8B) compared less well with observed Th_p activities, averaging only within 27% relative error. Partly this was due to analytical noise in the differencing technique used to estimate Th_p in Fig. 2B. The subsurface maximum in the distribution of modeled Th_t was the major feature of distribution of modeled Th_p. This subsurface maximum appeared in the data only at 2°S (Fig. 2C). The model Th_p subsurface maximum extended across all latitudes but was concentrated just north of the equator (0–1°) between the maximum in w at the equator (Fig. 3B) and the maximum in P at 2°N (Fig. 4). The surface low in Th_p was a consequence of the combination of the zero flux boundary condition at the surface and the parameterization of uniform sinking of Th_p. Neglecting the effects of advection and diffusion, model Th_p increased with depth from the surface to the depth where adsorption balanced decay, desorption and sinking (Eq. (2)). The addition of vertical diffusion and a mixed layer removed much of the depth structure. The subsurface maximum did not completely disappear as adsorption exceeds decay, desorption and sinking in the upper 100 m.

4.2. Comparison of ^{234}Th in the water column and in sediment traps

In this section we evaluate the degree to which the measured ^{234}Th deficiency reflected the sinking flux of ^{234}Th during EqPac Survey II and discuss the usefulness of the ^{234}Th method for sediment trap calibration in the presence of strong upwelling. As was discussed above, it has been proposed that the ^{234}Th deficiency is an accurate, independent measure of the sinking flux of ^{234}Th and can be compared with the measured ^{234}Th flux to calibrate sediment traps (Buesseler, 1991). The ^{234}Th fluxes expected from the observed (+) and modeled (O) ^{234}Th deficiencies alone in the upper 120 m are shown in Fig. 9A. These estimates agreed quite well (averaging within 10%). We found this very encouraging considering that our simple model used only minimal adjustable parameters, a single adsorption rate constant and sinking velocity, to fit the data. In the model, upwelling transported high ^{234}Th from depth. This led to an intense equatorial minimum in the deficiency. That this minimum was well displayed in the data (Fig. 9A) is supporting evidence that upwelling was indeed vigorous during EqPac Survey II.

Three estimates of the sinking flux of ^{234}Th at 120 m are shown in Fig. 9B: the ^{234}Th flux collected in sediment traps (Δ; Murray et al., 1996), the observed deficiency of total ^{234}Th from ^{238}U corrected for vertical and meridional advective fluxes (+) using velocities from Chai (1995) (Murray et al., 1996) and the model-derived sinking flux of ^{234}Th (O) expressed as the product of the sinking rate times the particulate ^{234}Th activity at 120 m ($= S\,Th_{p120}$). The magnitude of the model sinking flux (O) and the observed ^{234}Th deficiency corrected for advective fluxes (+; Murray et al., 1996) were quite similar, averaging within 17% and showing no significant positive or negative bias between them (Mann-Whitney U-test, $P > 0.10$; Sokal and Rohlf, 1995; Rohlf and Sokal, 1995). These two flux estimates showed similar meridional trends of

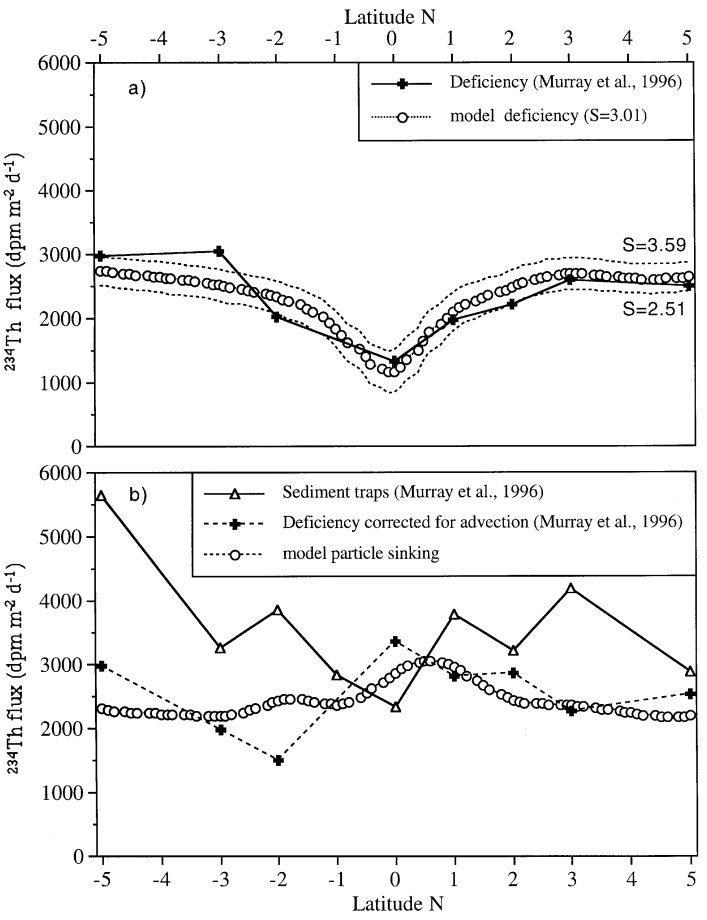

Fig. 9. Comparisons at 120 m between data from Murray et al. (1996) and model output for the ^{234}Th deficiency (A) and the ^{234}Th sinking flux (B). (A) compares the calculated ^{234}Th deficiency from Murray et al. (1996; filled crosses) with the model deficiency tuned to match the observation ($S = 3.01\ \mathrm{m\,d^{-1}}$; open circles) as well as the results for the 93% confidence interval for the sinking velocity ($S = 2.51\ \mathrm{m\,d^{-1}}$ to $S = 3.59\ \mathrm{m\,d^{-1}}$; dotted lines). (B) compares the measured ^{234}Th flux in sediment traps averaged between 100 and 150 m (open triangles; Murray et al. 1996), the calculated ^{234}Th deficiency corrected for advection (filled crosses; Murray et al. 1996) and the sinking flux from the model (open circles).

broad maxima near the equator, roughly mirroring the minima observed in Fig. 9A. The advection corrections made for the EqPac Survey II data (Murray et al., 1996) are thus consistent with their model predictions, suggesting that (1) advection can be estimated using observed ^{234}Th gradients and (2) that advection corresponds to a large fraction of the difference between the deficiency and the sinking flux.

The ^{234}Th method has shown that drifting sediment traps are often subject to intense biases (Buesseler, 1991). For the ^{234}Th method to be a useful calibrator of sediment traps, however, its own uncertainties must be less than the uncertainties in sediment

trap fluxes alone. The observed deficiency corrected for advection (+) and the model sinking flux (*O*) compared well and contrast with the sediment trap fluxes (Δ) in Fig. 9B. Sediment trap fluxes (Δ) were statistically higher than the model flux (*O*) by 27–59% (Mann-Whitney *U*-test, $P < 0.05$), averaging 32% higher. Over the whole region (5°N–5°S) Sediment trap fluxes (Δ) were also statistically higher than the deficiency corrected for advection (+) by 12–89% (Mann-Whitney *U*-test, $P < 0.05$), averaging 49% higher. Murray et al. (1996) used this comparison as evidence that Particle Interceptor Traps (PIT) overcollected ^{234}Th.

This consistency of the observed advection corrected ^{234}Th deficiency with the model ^{234}Th sinking flux, relative to the variability in the ^{234}Th trap fluxes, is support for calibrating trap fluxes using the ^{234}Th method. It suggests that processes behind ^{234}Th cycling were relatively homogenous over the entire EqPac Survey II transect and that the observed ^{234}Th deficiency can be adequately corrected for advection using observed gradients and estimates of v and w to give an accurate approximation of the true export of ^{234}Th. It should be noted that this is a necessary but not sufficient criterion for use of the ^{234}Th method for calibrating sediment traps. The other necessary criterion is that the ^{234}Th content of particles collected in sediment traps must be representative of the sinking material. This issue is discussed in detail elsewhere (e.g. Murray et al., 1996; Dunne et al., 1997).

4.3. *Sensitivity of ^{234}Th fluxes to the physical model*

To compare the relationship between the modeled ^{234}Th deficiency alone and the modeled sinking flux (the deficiency plus physical terms) in more detail, we present the ratio of deficiency flux: sinking flux at 120 m (R_{def}) as a function of latitude for a suite of model solutions using various combinations of advection and diffusion terms (Fig. 10). As in Fig. 6, results are for model runs in which combinations of advection and diffusion were switched on and off to illustrate their influence on calculated ^{234}Th fluxes given various hypothetical sets of conditions. Also shown is the ratio of the observed deficiency flux to the advection corrected deficiency flux for EqPac Survey II from Murray et al. (1996). R_{def} shows the coherence between the expected sinking flux of ^{234}Th and the ^{234}Th deficiency. Without advection or diffusion in the model ($\diamond$; same as Fig. 6A), R_{def} was identical to unity. With diffusion alone in the model (●; same as Fig. 6B), the deficiency still predicted the sinking flux within 2% at all latitudes. This is a situation characteristic of many areas of the open sea. With advection but no diffusion in the model (+, same as Fig. 6C), the combination of high ^{234}Th water upwelling from below and desorption of ^{234}Th from sinking particles resulted in negative values of R_{def} at the equator. This implies that in the absence of diffusion, not only would the ^{234}Th deficiency underestimate the sinking flux of ^{234}Th at the equator, but a super-equilibrium would exist. Model results with advection and either vertical diffusion (∇) or horizontal diffusion (Δ) suggested that both vertical and horizontal diffusion are important in mitigating this effect in the central equatorial Pacific. With all advection and diffusion processes incorporated into the model (+), R_{def} compared quite well with the ratio from Murray et al. (1996). The two estimates compared least well at 2–3°S where the

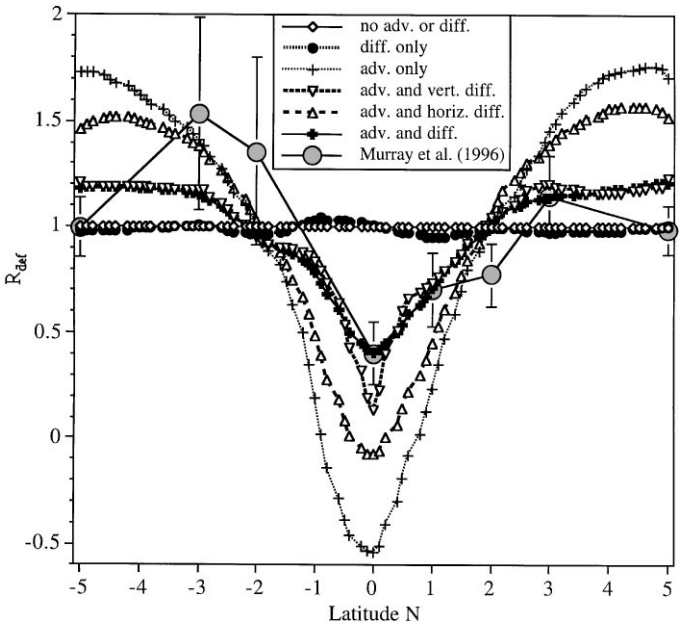

Fig. 10. Estimates of R_{def} for various hypothetical circulation scenarios: no advection or diffusion (open diamonds), diffusion only (filled circles), advection only (crosses), advection and vertical diffusion only (down-turned, open triangles), advection and horizontal diffusion only (up-turned, open triangles), with advection and diffusion (filled crosses) and data from Murray et al. (1996) (large, filled circles).

advection correction in Murray et al. (1996) was highly influenced by the zonal transition between the south equatorial countercurrent and the south equatorial current. Given that the model horizontal diffusion flux away from the equator was so large, it is surprising that the model and Murray et al. (1996) approximation agree so well at the equator. The uncertainty in the model advection and diffusion fluxes and their sensitivity to the scavenging model is further discussed below.

As shown in Fig. 10, upwelling in the central equatorial Pacific can have a large effect on the accuracy of the ^{234}Th deficiency as an indicator of the ^{234}Th sinking flux. Because the strength of upwelling varies considerably in the central equatorial Pacific, we decided to assess the affect of this variability on the accuracy of the ^{234}Th method by varying the magnitude of the model advection field. We present model results for the ratio of the deficiency flux to the sinking flux (R_{def}; Fig. 11A) and the ratio of the deficiency flux corrected for advection to the sinking flux ($R_{def+adv}$; Fig. 11B) versus latitude for a range of magnitudes of equatorial upwelling. In addition to the simulation for the conditions of EqPac Survey II with upwelling at the base of the euphotic zone (w_{120}) at 1 m d^{-1}, we show simulations with $w_{120} < 1$ m d^{-1} (thin, gray lines) to simulate weaker upwelling and $w_{120} > 1$ m d^{-1} (thin, black lines) to simulate stronger upwelling. Model results suggest that the ^{234}Th deficiency alone underestimated ^{234}Th sinking flux by 144% at the equator (Fig. 11A). Furthermore, model results

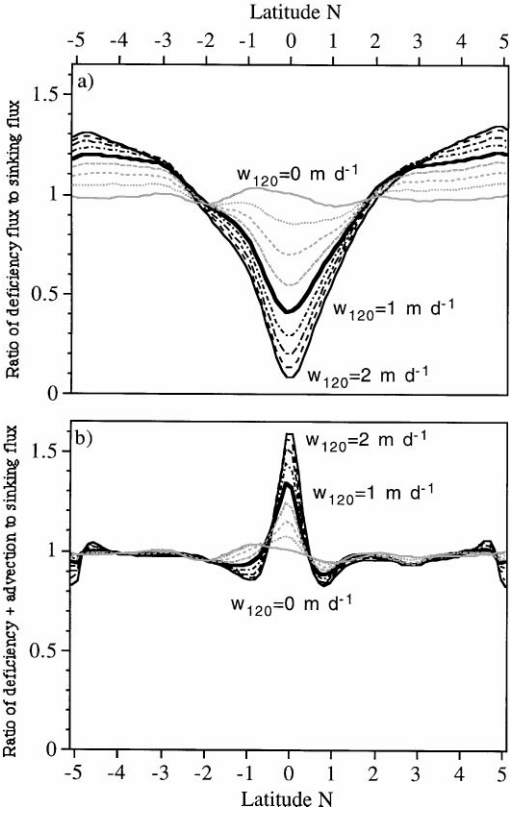

Fig. 11. Model results for R_{def} (A) and $R_{def+adv}$ (B) versus latitude. Curves are results for relative strength of advection between upwelling velocities at the equator at $0.25\,m\,d^{-1}$ increments from $0\,m\,d^{-1}$ (gray) through the chosen strength of $1\,m\,d^{-1}$ (thick black) to twice the chosen value ($2\,m\,d^{-1}$; black).

suggest that the ^{234}Th deficiency corrected for advection overestimated the ^{234}Th sinking flux by about 33% at the equator due to the important role of horizontal diffusion in transporting recently upwelled waters away from the equator. Fig. 11 shows that during conditions of relative mild upwelling, there is better agreement between the ^{234}Th deficiency and the ^{234}Th sinking flux, and thus the potential accuracy of the ^{234}Th method improves dramatically. Conversely, when upwelling is stronger than observed during EqPac Survey II, the ^{234}Th deficiency so drastically underestimates the sinking flux of ^{234}Th that the ^{234}Th method of calibrating sediment traps is based almost exclusively on the ^{234}Th advective and diffusive balance which is poorly constrained. Under these hypothetical conditions of vigorous upwelling, the ^{234}Th method has very limited utility. Using these results as a basis for evaluating the ^{234}Th method, we argue that the ^{234}Th method was successfully applied to calibrate sediment traps during EqPac Survey II, but that situations having upwelling velocities at the base of the euphotic zone greater than $1\,m\,d^{-1}$ would

prohibit use of the ^{234}Th method of estimating particle export within a reasonable uncertainty (factor of 2).

4.4. Sensitivity to the scavenging model

We chose the chemical scavenging model of Bacon and Anderson (1982, Fig. 1) for this analysis from the variety of models described in the literature (see comparison in Dunne et al., 1997) because of its simplicity. Circulation affects the ^{234}Th balance through the ^{234}Th gradients (Eqs. (1) and (2)). As these gradients are a manifestation of particle scavenging, it is important to consider uncertainties in the scavenging model to understand the role of circulation on the ^{234}Th flux balance. Sources of potential variability lie in both the adsorption and sinking parameterizations.

Given the assumptions in the scavenging model of a first-order inherent adsorption rate constant ($k_1' = k_1 P$) and a homogeneously sinking particle pool, the data constrain estimates of k_1 and S quite well, resulting in little variability in R_{def} and $R_{\mathrm{def+adv}}$ (Fig. 12). Uncertainty in the magnitude of k_1 (Fig. 5) had very little effect on R_{def} and $R_{\mathrm{def+adv}}$. The 95% confidence limits on k_1 (0.0266–0.0343 m^3 mmol C^{-1} d^{-1}) translated into a negligible 1% relative uncertainty in R_{def} at the equator. Uncertainty in the sinking velocity parameterization translated to a larger variability in R_{def} and

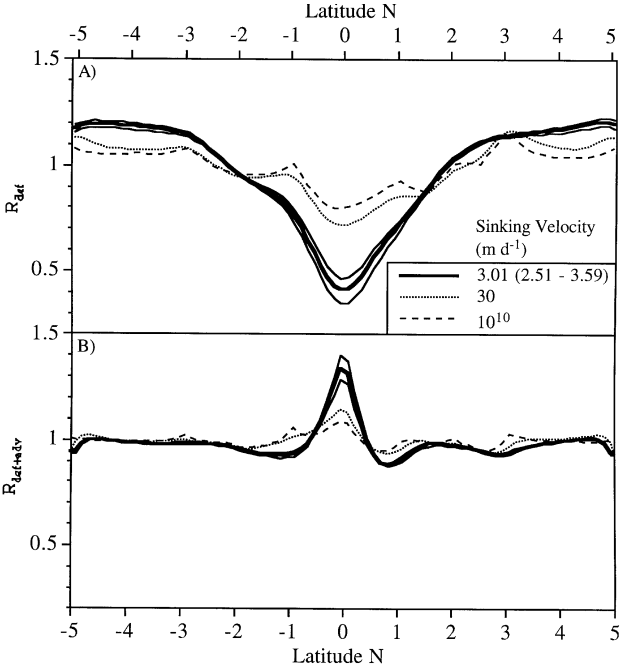

Fig. 12. Model results for R_{def} (A) and $R_{\mathrm{def+adv}}$ (B) under various scenarios: the sinking velocity tuned to the observed deficiency $S = 3.01\ \mathrm{m\,d^{-1}}$ (thick, solid line) with its upper ($S = 3.59\ \mathrm{m\,d^{-1}}$; thin, solid line) and lower ($S = 2.51\ \mathrm{m\,d^{-1}}$; thin, solid line) 93% confidence limits, the case of rapidly sinking particles of $S = 30\ \mathrm{m\,d^{-1}}$ (dotted line) and with S approaching infinity ($S = 10^{10}\ \mathrm{m\,d^{-1}}$; dashed line).

$R_{\mathrm{def+adv}}$ and is shown in Fig. 12. The 95% confidence limits on S (2.51–3.59 m d^{-1}) translated to a 7% relative uncertainty in R_{def} at the equator. This uncertainty was slightly smaller than the uncertainty in the deficiency itself, which averaged 9% during EqPac Survey II (Murray et al., 1996) and much less than the total uncertainty due to the uncertainty in the advective component.

The first mechanistic assumption of the scavenging mechanism (Fig. 1) is that ^{234}Th adsorption to particles can be parameterized as a first order reaction between dissolved ^{234}Th and the particle concentration. There is some evidence that the order of the reaction is less than one due to a "particle concentration effect" (Honeyman et al., 1987). To understand the model sensitivity to the reaction order, we re-parameterized k_1' using the reaction order (b) as a free parameter (i.e. $k_1' = k_1 P^b$). We found that the data constrained the 95% confidence interval of the reaction order to between $b = 0.68$ (giving $k_1 = 0.0321$) and $b = 1.27$ (giving $k_1 = 0.02925$). This uncertainty in the adsorption parameterization translated to a 10% relative uncertainty in R_{def} at the equator. Again, this uncertainty was of similar magnitude to the uncertainty in the measured deficiency itself.

The second mechanistic assumption of the scavenging mechanism (Fig. 1) is that ^{234}Th export is dominated by slow sinking of relatively common, small particles. Effectively, slow sinking velocity was used to parameterize particle processes such as repackaging and aggregation that convert suspended particles into sinking ones. In addition, this assumption allowed us to constrain the model using the dissolved ^{234}Th data. Alternatively, if particle processes in the central equatorial Pacific were relatively instantaneous and ^{234}Th scavenging was limited by adsorption alone, ^{234}Th export would be dominated by the rapid sinking of relatively rare, large particles (Dunne et al., 1997). We investigated this potential scavenging mechanism by re-parameterizing k_1 and S under the assumption that the sinking flux was dominated by rare, rapidly sinking particles. Data on total ^{234}Th was assumed to represent non-sinking ^{234}Th only ($Th_{\mathrm{d}} \approx Th_{\mathrm{t}}$), and the concentration of ^{234}Th on rapidly sinking particles was initially assumed negligible ($\mathrm{Th_p} \approx 0$). We first re-calculated k_1' values from the total ^{234}Th data using Eq. (3). We then recalculated k_1 ($= 0.0089$ mmol C^{-1} m^3 d^{-1}) from the slope of k_1' versus P as before using Mood's method. Finally, we recalculated S ($= 30$ m d^{-1}) as before from the observed deficiency.

This scavenging mechanism gave ^{234}Th distributions (Fig. 13A) with dramatically different vertical and meridional structure than did the first mechanism. A diagnostic summary of the ^{234}Th flux balance between 0 and 120 m is shown in Fig. 13B. Compared to the mechanism of slowly sinking particles, the mechanism of rapidly sinking particles gave activities of total ^{234}Th slightly closer to the data (on average within 8%) but reproduced slightly less of the variability in the data (73%). ^{234}Th activities were much lower at depth than before, well below equilibrium with ^{238}U. We attribute this to the relative efficiency of particle sinking relative to desorption and decay in this mechanism. The mechanism of rapidly sinking particles also showed much less meridional structure in ^{234}Th near the surface than either the data or the mechanism of slowly sinking particles.

The scavenging mechanism of rapidly sinking particles gave values of R_{def} that clustered much more tightly about unity (gray, dotted line, Fig. 12), implying that

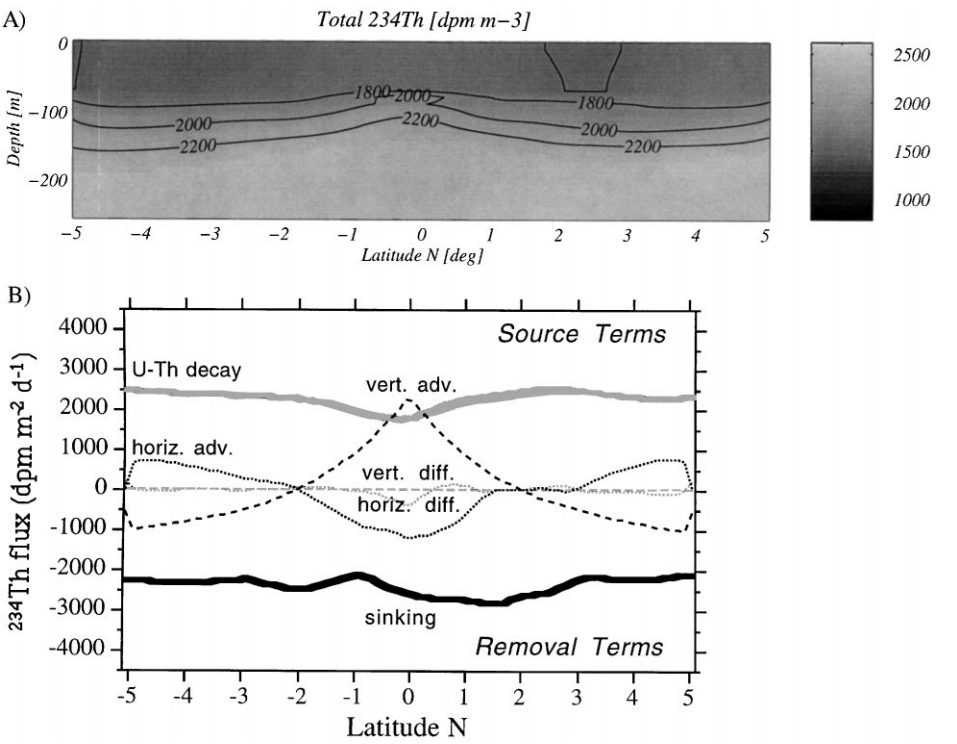

Fig. 13. Model contours of total ^{234}Th (A) (dpm m^{-3}) between 5°N and 5°S in the upper 250 m using the scavenging mechanism of rapidly sinking particles ($k_1 = 0.0089$ mmol C^{-1} m^3 d^{-1}; $S = 30$ m d^{-1}). Model diagnostic summary of the ^{234}Th flux balance (0–120 m) versus latitude (B) using this same scavenging mechanism.

the ^{234}Th deficiency would be approximately twice as accurate a predictor of the ^{234}Th sinking flux if particle processes (e.g. aggregation and repackaging) were instantaneous and sinking was dominated by rare, rapidly sinking particles. In Fig. 12, we also show the hypothetical case in which the sinking velocity approaches infinity ($S = 10^{10}$). As the sinking velocity approaches infinity, R_{def} approaches not 1.00 but a value less than 1.00, limited by the rate of adsorption and circulation of Th_{d}.

This sensitivity of R_{def} to the scavenging mechanism makes it important to distinguish which scavenging mechanism is more appropriate. Firstly, the mechanism of slowly sinking particles gave ^{234}Th deficiencies which were on average within 10% of the observed deficiency and within 12% at the equator. ^{234}Th deficiencies from the rapidly sinking particle model were on average within only 15% of the observed deficiency and within only 35% at the equator. Secondly, meridional advection was a large term at the equator (-1187 dpm m^{-2} d^{-1}) for the scavenging mechanism of rapidly sinking particles (Fig. 13B). This was much higher than the meridional fluxes of ^{234}Th at the equator calculated by Murray et al. (1996; -108 ± 65 dpm m^{-2} d^{-1}) and Buesseler et al. (1995; ~ 0 dpm m^{-2} d^{-1}) and in the model with slowly sinking

particles ($-158\ \mathrm{dpm\,m^{-2}\,d^{-1}}$). The large meridional flux of ^{234}Th away from the equator at the surface in the model of rapidly sinking particles is not balanced by high ^{234}Th transported meridionally towards the equator near the base of the euphotic zone, because the ^{234}Th activities at this depth are relatively low. Given these two pieces of evidence, we suggest that the scavenging model with slowly sinking particles was more representative of euphotic zone scavenging in the central equatorial Pacific, as it predicted only moderate meridional fluxes of ^{234}Th from the equator (Fig. 7). It is important to note that these results suggest only that there is a timescale associated with particle processes (e.g. repackaging, aggregation) in the central equatorial Pacific and not that all particles necessarily sink slowly at all depths. Indeed, the good comparison of the data and the model with rapidly sinking particles at depths below the euphotic zone suggests that particle sinking may be dominated by rapidly sinking particles in this region. This analysis showed that R_{def} is very sensitive to the nature of the particle removal process and that the deficiency is a much more accurate predictor of the sinking flux under conditions of rapid particle processing and sinking.

4.5. *Overall uncertainty in R_{def} and $R_{\mathrm{def+adv}}$*

To gauge the overall accuracy of calculated ^{234}Th sinking fluxes during EqPac Survey II, we estimated the uncertainty in R_{def} and $R_{\mathrm{def+adv}}$ using the Monte-Carlo Bootstrapping technique of error propagation (Bevington and Robinson, 1992; Press et al., 1992). Uncertainty in all input parameters was propagated through the model to obtain 95% confidence intervals on R_{def} and $R_{\mathrm{def+adv}}$ (Fig. 14). The error in k_1 and S was assumed to be normally distributed ($\sigma_{k1} = 0.001925\ \mathrm{mmol\,C\,m^{-3}\,d^{-1}}$; $\sigma_S = 0.29\ \mathrm{m\,d^{-1}}$). Relative standard deviations of 50% were assumed for the v and w fields (F. Chai, personal communication). We assumed the uncertainty in diffusion constants to be exponentially distributed about the chosen value to approximate the skew in the range of values in the literature discussed above. This assumption gave 95% confidence intervals of 0.04–2.22 $\mathrm{cm^2\,s^{-1}}$ for K_z (below the euphotic zone only) and 135–7390 $\mathrm{m^2\,s^{-1}}$ for K_{h}. The Monte-Carlo Bootstrapping routine then picked 5000 cases of input parameters based on these uncertainties to obtain 5000 estimates of R_{def} and $R_{\mathrm{def+adv}}$.

Results of this analysis showed that uncertainty in both R_{def} and $R_{\mathrm{def+adv}}$ was large at the equator. The 95% confidence intervals for both R_{def} (Fig. 14A) and $R_{\mathrm{def+adv}}$ (Fig. 14B) spanned from unity to approximately twice the median value. This uncertainty was dominated by the uncertainty in the terms for advection and horizontal diffusion. At the equator, uncertainty in R_{def} suggests that the sinking flux may have been up to 5 times greater than the deficiency would predict. This uncertainty implies that the ^{234}Th method cannot be used to calibrate sediment traps at the equator without correcting the calculated ^{234}Th flux for advection. Uncertainty in $R_{\mathrm{def+adv}}$ suggests that accounting for advection but not diffusion overestimates the sinking flux by up to 63% at the equator and underestimates the flux by 0–23% off the equator. When a similar analysis was performed using the scavenging mechanism of rapid particle sinking, 95% confidence intervals shrank considerably about unity but kept the same overall shape as in Fig. 14. In general, this analysis confirmed the

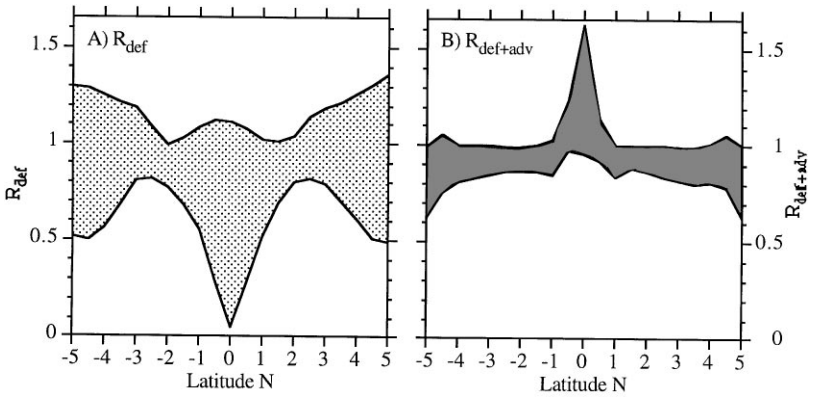

Fig. 14. 95% confidence intervals on R_{def} (A) and $R_{def+adv}$ (B) obtained from the Monte-Carlo Bootstrapping method (Bevington and Robinson, 1992; Press et al., 1992).

viability of using the ^{234}Th deficiency corrected for advection as a measure of the sinking flux of ^{234}Th and as a means of calibrating sediment traps. Within one degree of the equator, however, these estimates may have biases up to 50% due to the role of horizontal diffusion.

5. Conclusions

We coupled a chemical scavenging model with a simple physical model of equatorial circulation to investigate the impact of circulation on calculations of the ^{234}Th export flux. We assumed adsorption to be first order with respect to both dissolved ^{234}Th and particle concentration ($k_1 = 0.2905\ \mathrm{mmol\,C^{-1}\,m^3\,d^{-1}}$). The sinking velocity was adjusted to a single value of $3.01\ \mathrm{m\,d^{-1}}$. The model reproduced both the meridional trend in the observed ^{234}Th deficiency of relatively low ^{234}Th deficiencies near the equator and the depth structure observed for total and dissolved ^{234}Th. Model results illustrated the importance of a mixed layer in reproducing observed total ^{234}Th distributions.

The model sinking flux of ^{234}Th compared well with the observed ^{234}Th deficiency corrected for advection (Murray et al., 1996) relative to the measured sediment trap fluxes of ^{234}Th (Murray et al., 1996), which were found to be relatively erratic and high. This illustrated the high level of internal consistency in ^{234}Th method between predicted and observed fluxes necessary for its use to calibrate sediment traps.

Analysis of the model physics illustrated the importance of advection in the ^{234}Th flux balance in the equatorial surface layer. This study confirms that upwelling at the equator has a dramatic impact on the applicability of the ^{234}Th method for particle export calculation. However, our results point to a significant role of horizontal diffusion in mitigating the effect of vertical advection on ^{234}Th fluxes at the equator such that the ^{234}Th deficiency corrected for advection overestimated

the ^{234}Th sinking flux by 33% in neglecting horizontal diffusion. Nevertheless, this potential bias in the estimates of Buesseler et al. (1995) and Murray et al. (1996) and Bacon et al. (1996) is within the original published uncertainties of $\sim 60\%$. Vertical mixing was shown to be a negligible ^{234}Th flux across 120 m. A model sensitivity analysis to the strength of equatorial upwelling showed that the ^{234}Th deficiency would be only a small component of the total ^{234}Th balance under conditions of upwelling stronger than those estimated for the EqPac Survey II, implying that uncertainty in the sinking flux of ^{234}Th would be very large under these conditions and application of the ^{234}Th method would be ill-advised.

A sensitivity analysis of the scavenging mechanism used in the model showed that the ratio of the ^{234}Th deficiency to the ^{234}Th sinking flux (R_{def}) was insensitive to the uncertainty of k_1 and S, which are well constrained by the data. Investigation of other potential sinking mechanisms suggested that if ^{234}Th export were governed by rare, rapidly sinking particles, it would have been only about half as sensitive to advection than if it were governed by slowly sinking particles. This suggested that the ^{234}Th deficiency would be an accurate predictor of the ^{234}Th sinking flux during particle aggregation and rapid sinking (e.g. phytoplankton blooms) even in fairly vigorous physical regimes. Because the scavenging mechanism of slowly sinking particles compared better with the observed ^{234}Th deficiency and calculated meridional ^{234}Th fluxes at the equator than the mechanism of rapidly sinking particles, we suggested that the slowly sinking particle mechanism was more appropriate for the central equatorial Pacific.

Propagation of uncertainty through the model further illustrated the large uncertainty in the ^{234}Th method at the equator. Results suggested that the ^{234}Th deficiency underestimated the ^{234}Th sinking flux by 1–612% ($P = 0.05$) while advection corrected estimates overestimated the ^{234}Th sinking flux by 0–63% ($P = 0.05$) because they neglected horizontal diffusion. In general, comparison of model results with observations from Murray et al. (1996) confirmed that in this dynamic regime, the ^{234}Th deficiency corrected for advection was successfully used to measure of the sinking flux of ^{234}Th and improved the accuracy of sediment traps.

Acknowledgments

We thank Mitsuhiro Kawase, Laurie Balistrieri, Steve Emerson, Bruce Frost and two anonymous reviewers for helpful comments and criticism. This research was supported by NSF grant OCE 9022466 and NASA Global Change (Earth System Science) Fellowship # 1995-GlobalCh00307. School of Oceanography Contribution Number 2195. US JGOFS Contribution Number 447.

References

Bacon, M.P., Anderson, R.F., 1982. Distributions of thorium isotopes between dissolved and particulate forms in the deep sea. Journal of Geophysical Research 87(C3), 2045–2056.

Bacon, M.P., Cochran, J.K., Hirshberg, D., Hammar, T.R., Fleer, A.P., 1996. Export fluxes of carbon at the equator during the EqPac time-series cruises estimated from ^{234}Th measurements. Deep Sea Research II 43, 1133–1154.

Bevington, P.R., Robinson, D.K., 1992. Data Reduction and Error Analysis for the Physical Sciences, 2nd ed. McGraw-Hill, New York, pp. 75–83.

Bishop, J.K.B., 1998. Particulate organic carbon/particulate dry weight and beam attenuation coefficient measurements, Deep-Sea Research I (in press).

Buesseler, K.O., 1991. Do upper-ocean sediment traps provide an accurate indicator of particle flux? Nature 353, 420–423.

Buesseler, K.O., Bacon, M., Cochran, J.K., Livingston, H., 1992. Carbon and nitrogen export during the JGOFS North Atlantic Bloom Experiment estimated from ^{234}Th : ^{238}U disequilibria, Deep-Sea Research 39, 1115–1137.

Buesseler, K.O., Michaels, A.F., Siegel, D.A., Knap, A.H., 1994. A three dimensional time-dependent approach to calibrating sediment trap fluxes. Global Biogeochemical Cycles 8, 179–193.

Busseler, K.O., Andrews, J., Hartman, M., Belastock, R., 1995. Regional estimates of the export flux of particulate organic carbon derived from thorium-^{234} during the JGOFS EQPAC program. Deep-Sea Research II 42, 777–804.

Clegg, S.L., Whitfield, M., 1993. Application of a generalized scavenging model to time series ^{234}Th and particle data obtained during the JGOFS North Atlantic Bloom Experiment. Deep-Sea Research I 40, 1529–1545.

Chai, F., 1995. Origin and mainainance of high nitrate condition in the equatorial Pacific, a biological-physical model study. Ph.D. Dissertation, Duke University, Durham, NC, 170pp.

Coale, K.H., Bruland, K.W., 1985. ^{234}Th : ^{238}U disequilibria within the California current. Limnology and Oceanography 30, 22–33.

Dunne, J.P., Murray, J.W., Young, J., Balistrieri, L., Bishop, J.K.B., 1997. ^{234}Th and particle cycling in the central equatorial Pacific. Deep Sea Research II 44, 2049–2083.

Dunne, J.P., Murray, J.W., Rodier, M., Hansell, D.A. (submitted) Export production in the western and central equatorial Pacific: zonal and temporal variability. Deep-Sea Research I.

Fine, R.A., Ostlund, H.G., 1980. Exchange times in the Pacific equatorial current system. Earth and Planetary Research Letters 49, 447–452.

Gardener, W.D., Chung, S.P., Richardson, M.J., Walsh, I.D., 1995. The oceanic mixed layer pump. Deep-Sea Research II 42, 757–776.

Honeyman, B.D., Balestrieri, L.S, Murray, J.W., 1988. Oceanic trace metal scavenging: the importance of particle concentration. Deep-Sea Research 35, 227–246.

Ledwell, J.R., Watson, A.J., Law, C.S., 1993. Evidence for slow mixing across the pycnocline from an open-ocean tracer-release experiment. Nature 364, 701–703.

Liu, Z., Philander, S.G.H., Pacanowski, R.C., 1994. A GCM study of tropical-subtropical upper-ocean water exchange. Journal of Physical Oceanography 24, 2606–2623.

Lu, P., McCreary Jr. J.P., Klinger, B.A., 1998. Meridional circulation cells and the source waters of the Pacific Equatorial Undercurrent. Journal of Physical Oceanography 28, 62–84.

Mood, A.M., 1950. Introduction to the Theory of Statistics. McGraw-Hill, New York.

Munk, W.H., 1966. Abyssal recipes. Deep-Sea Research 13, 707–730.

Murray, J.W., Barber, R.T., Roman, M.R., Bacon, M.P., Feely, R.A., 1994. Physical and biological controls on carbon cycling in the equatorial Pacific. Science 266, 58–65.

Murray, J.W., Young, J., Newton, J., Dunne, J.P., Chapin, T., Paul, B., 1996. Export production determined using ^{234}Th : ^{238}U disequilibria. Deep-Sea Research II 43, 1095–1132.

Pacanowski, R.C., Philander, S.G.H., 1981. Parameterization of vertical mixing in numerical models of tropical oceans. Journal of Physical Oceanography 11, 1443–1451.

Press, W.H., Teukolky, S.A., Vetterling W.T., Flannery, B.P., 1992. Numerical Recipes in FORTRAN, 2nd ed. Cambridge University Press, Cambridge.

Rohlf, F.J., Sokal, R.R., 1995. Statistical Tables, 3rd ed. W.H. Freeman and Co., New York.

Sokal, R.R., Rohlf, F.J., 1995. Biometry, 3rd ed. W.H. Freeman, New York.

Wyrtki, K., Kilonsky, B., 1984. Mean water and current structure during the Hawaii-Tahiti Shuttle Experiment. Journal of Physiccal Oceanography 14, 242–254.